

# From Benzene to Graphene: Exploring the Electronic Structure of Single-Layer and Bilayer Graphene Using Polycyclic Aromatic Hydrocarbons

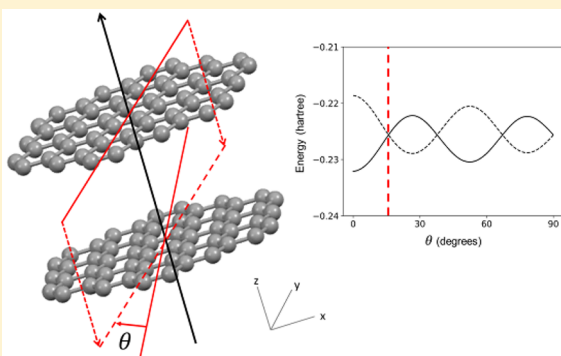
Janna Domenico,<sup>id</sup> Alexis M. Schneider,<sup>† id</sup> and Karl Sohlberg<sup>\* id</sup>

Department of Chemistry, Drexel University, Philadelphia, Pennsylvania 19104-2875, United States

## Supporting Information

**ABSTRACT:** In this work, two exercises are described that are designed to teach students about the evolution and behavior of the electronic bands of graphene and bilayer graphene. These exercises involve performing extended Hückel molecular orbital theory calculations on polyacenes and polycyclic aromatic hydrocarbons. In the first exercise, students investigate how the molecular orbitals of polyacenes converge into bands as polyacene size increases. Further, students learn that long-range interactions cause frontier-orbital crossing as the size of the polyacene increases. In the second exercise, the concepts of band structures, band crossing, and  $k$ -space are explored using the results of frontier orbital calculations on  $\pi$ -stacked dimers of polycyclic aromatic hydrocarbons, which represent molecular analogues of layered 2D materials. The results of these calculations show how the geometry and layer–layer offset of the dimer system can affect its electronic structure, and the results can be extrapolated to provide a framework for understanding why subtle changes in the relative orientations of the layers in bilayer graphene can produce qualitative changes in the electronic properties. These calculations are easily implemented with Python or with widely available algebraic manipulation software such as Maple or Mathematica. These exercises are accessible to students who have experience with extended Hückel molecular orbital theory and are suitable for inclusion in the physical chemistry curriculum at the upper-level undergraduate or introductory graduate level.

**KEYWORDS:** Upper-Division Undergraduate, Graduate Education/Research, Physical Chemistry, Computer-Based Learning, Theoretical Chemistry, Materials Science, MO Theory



## INTRODUCTION

Graphene, isolated in 2004,<sup>1</sup> is an intriguing modern material consisting of a single sheet of hexagonally arranged carbon atoms. It represents the theoretical limit of size reduction in at least one spatial dimension because it is just one atom thick in the direction normal to the plane of the sheet. The discovery of graphene has spawned tremendous interest in such “2D materials”,<sup>2</sup> especially for potential applications in electronic devices, because these materials promise to make possible the ultimate reduction of feature size in electronic device elements. Applications are also envisioned in biomedical science,<sup>3</sup> separations science,<sup>4</sup> and photoenergy conversion.<sup>5</sup> With such enormous technological significance, 2D materials and especially graphene as the archetype thereof deserve a prominent place in the chemistry curriculum.

For pedagogical purposes, to instill a conceptual understanding of graphene’s electronic structure, it is desirable that students be able to relate it to established chemical concepts. Among chemists, a widely used model of electronic structure is the orbital picture. Electrons are thought of as filling and occupying orbitals according to the aufbau and Pauli principles; the electronic structures of large systems are

described by taking linear combinations of the orbitals of their smaller subsystems. This is the starting point for the present exploration of the electronic structure of graphene. The electronic bands of graphene are introduced as the asymptotic limit of the molecular orbitals (MOs) of polyacenes; the MOs of polyacenes are taken to be linear combinations of carbon atomic orbitals (AOs).

Herein, two exercises are described that are designed to help students in upper-level undergraduate or introductory-graduate level courses achieve learning goals associated with materials chemistry concepts. Because extended Hückel MO theory (EHT) is used, these exercises are ideal for students who have been exposed to quantum mechanics. The EHT model of electronic structure is consistent with the above-described physical picture of electronic structure that chemists carry around in their mind’s eye and is simultaneously sufficiently mathematically simple that students can perform the requisite calculations without recourse to “canned” quantum chemistry

Received: April 10, 2019

Revised: August 20, 2019

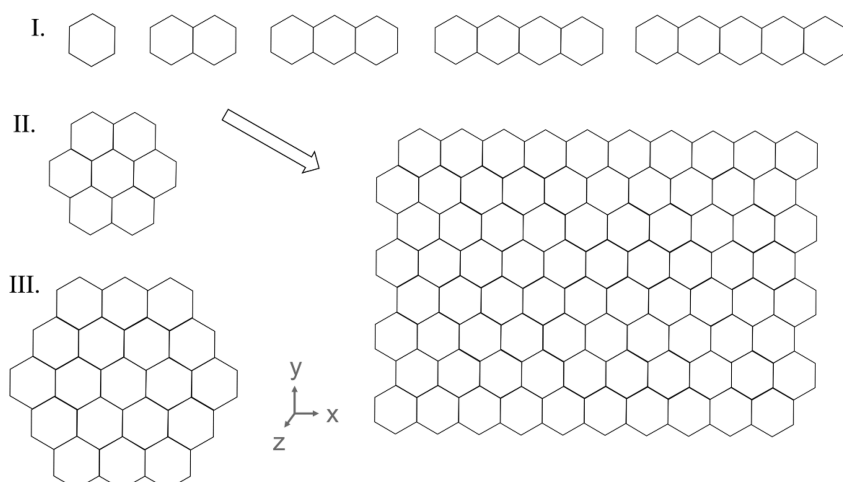


**Figure 1.** Evolution of polyacenes from benzene (top row) and selected PAHs (left column). Hydrogen and double bonds are redacted for clarity. Note that another layer can be added along the *z*-axis to portray the bilayer analogues of these systems.

software. Such codes can obscure the chemical and mathematical insights within the “black box” of the software. These features render EHT an excellent choice for educational purposes. Indeed, it has history of application in the chemical education community. It has been used to teach about the mechanism of covalent bonding,<sup>6</sup> the concept of a maximum wavelength of absorbance of dyes,<sup>7</sup> and the origin of Jahn–Teller distortion.<sup>8</sup> By developing an atomic and molecular level understanding of the electronic structure of graphene, students of chemistry will be preparing themselves for technical careers in a world that sees widespread use of 2D and nanomaterials, especially in electronic applications.<sup>9</sup>

The exercises described herein can be carried out using Python or symbolic algebra software such as Maple<sup>10</sup> or Mathematica.<sup>11</sup> These exercises can be used to teach students about the origin of band theory, to introduce the electronic structure of graphene and similar materials, to reinforce key concepts in quantum mechanics, and also to highlight the importance of programming skills to those interested in computational science.

This work has the potential for three “levels” of incorporation in an undergraduate or graduate physical chemistry course: (1) having students perform each exercise independently or in teams as one or multiple homework assignments, (2) having students perform the truncated versions of these exercises described in the penultimate section below, or (3) using the results of these exercises as the contents of a lecture with no need to assign work to the students. For the convenience of such an instructor, lecture slides are included as [Supporting Information](#).

Students who perform these exercises or attend a lecture based on this content are expected to achieve the following four learning outcomes:

- (1) Infer whether graphene is a conductor, insulator, or semiconductor by extrapolation from the electronic structures of a series of polyacenes of increasing size.
- (2) Demonstrate the effect of long-range interactions on the HOMO–LUMO gap of a polyacene system.
- (3) Deduce the presence of orbital crossings in polyacenes from the system-size dependence of the HOMO and LUMO energies.
- (4) Connect the relative energies of two stacked orbitals to the concepts of bandwidth and *k*-space.

## POLYACENES AND POLYCYCLIC AROMATIC HYDROCARBONS TO REPRESENT GRAPHENE

Graphene, like benzene, has a conjugated  $\pi$ -bonding structure, and this conjugation extends throughout the entire sheet. The extended conjugation is thought to facilitate electron transport and be at least partially responsible for the fact that graphene is a good conductor of electricity.<sup>12</sup> That very same high conductivity renders graphene a poor choice for semiconductor device fabrication, however, so chemical or structural modifications are needed before the material can be used in semiconductor applications.

Graphene can be thought of as the two-dimensional asymptotic limit of polyacenes, a class of hydrocarbons composed of linearly fused benzene rings, and further of polycyclic aromatic hydrocarbons (PAHs). The latter class of molecules is sometimes referred to as “nanographenes”.<sup>13</sup> It follows that one way to gain some insight into graphene’s electronic structure is to look at the evolution of  $\pi$ -bonding in polyacenes and PAHs with increasing size. The first exercise is designed to help students investigate the evolution of the electronic structure of polyacenes with increasing size (see Figure 1, row I) in order to extrapolate the findings to graphene.

Layered 2D materials are also appealing choices for devices, because the extra dimension offers an opportunity to tune the electronic structure.<sup>14</sup> In a second exercise, the EHT analysis is extended to stacked dimers of polyacenes and related PAHs (see Figure 1, structures II and III), which are molecular analogues of bilayer graphene. The exercise yields insight into the behavior of the valence bands of bilayer graphene and, by extension, the tunability of layered 2D materials.

These exercises serve as a vehicle to explore the origin of band structure and the reason why graphene is not a good semiconductor. Close inspection of the evolution of the energy levels reveals oscillatory behavior in the highest occupied molecular orbital (HOMO)–lowest unoccupied molecular orbital (LUMO) gaps of polyacenes. This behavior is indicative of curve crossings in frontier orbitals,<sup>13</sup> which has important implications for the band structure of graphene. Further, it was recently discovered that the electronic structure of bilayer graphene is sensitive to subtle structural changes.<sup>15</sup> These exercises are designed to give students insight into the

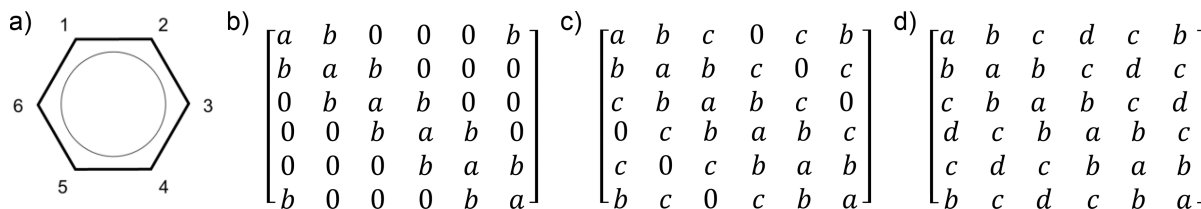


**Figure 2.** (a) Structure with atom numbers and (b) first-nearest-neighbor; (c) first- and second-nearest-neighbor; and d) first-, second-, and third-nearest-neighbor interaction matrices for benzene.

geometric and electronic structure aspects of graphene and bilayer graphene that are behind these behaviors.

## EXERCISE I: CREATING ENERGY LEVEL DIAGRAMS AND OBSERVING TRENDS

### Exercise I Background

The first student exercise described here is the use of EHT to observe the evolution of the electronic structure of polyacenes as the system grows in number of rings ( $M$ ) from  $M = 1$  to  $M = 100$ , the results of which can introduce students to the bands of graphene. First, EHT is reviewed in the context of this exercise.

To obtain molecular orbitals for the polyacenes, one starts from the time-independent Schrödinger equation:

$$\hat{H}\Psi = E\Psi \quad (1)$$

where  $\hat{H}$  is the Hamiltonian (total energy) operator,  $\Psi$  is the wave function, and  $E$  is the total energy of the system. By expanding  $\Psi$  in a basis of functions  $\chi_i$ :

$$\Psi = \sum_i c_i \chi_i \quad (2)$$

eq 1 can be recast as a linear algebra expression:<sup>16</sup>

$$\sum_i c_i (H_{ij} - ES_{ij}) = 0 \quad (3)$$

or in matrix notation

$$\mathbf{HC} = \mathbf{ESC} \quad (4)$$

where  $H_{ij}$  and  $S_{ij}$  are elements of matrices  $\mathbf{H}$  and  $\mathbf{S}$ . To construct matrices  $\mathbf{H}$  and  $\mathbf{S}$ , first, one selects a set of AOs,  $\chi_i$ , to form the basis set of the molecule of interest. Because the frontier orbitals in a polyacene are known to be of  $\pi$ -type,<sup>17</sup> an appropriate basis is a set of carbon 2p<sub>z</sub> orbitals, one on each carbon atom, all of which are taken to lie in the  $x$ - $y$  plane. This choice of basis effectively renders the calculation a  $\pi$ -EHT calculation. Then, the elements of  $\mathbf{H}$  are given by

$$H_{ij} = \int \chi_i^* \hat{H} \chi_j \, d\tau \quad (5)$$

EHT is implemented by using the following Mulliken–Wolfsberg–Helmholtz (MHW) approximations for the elements of the  $\mathbf{H}$  matrix:<sup>18</sup>

$$H_{ii} = -\text{VOIE}(\chi_i) \quad (6)$$

$$H_{ij} = 1.75 S_{ij} H_{ii} \quad (7)$$

where VOIE denotes valence orbital ionization energy, that is, the ionization energy of an electron in a  $\chi_i$  orbital on an isolated atom of the corresponding element. In the case of a carbon 2p orbital, this value is  $-10.77$  eV.<sup>16</sup> The subscript  $ii$

denotes the diagonal elements of such a matrix, and  $ij$  describes the interatomic interactions, which are off-diagonal elements.

The elements of  $\mathbf{S}$  (overlap integrals) are of the form

$$S_{ij} = \int \chi_i^* \chi_j \, d\tau \quad (8)$$

The  $\mathbf{S}$  elements are dependent upon the geometry of the system. Given that all the carbon atoms of the polyacene are taken to lie in the  $x$ - $y$  plane, the overlap of two p<sub>z</sub> orbitals is exclusively of  $\pi$  type. Analytic expressions are available for the  $\pi$ -overlap integral between functions of p-type:<sup>19</sup>

$$S_{ii} = 1 \quad (9)$$

$$S_{ij}^{pp_\pi} = \left( 1 + \zeta R_{ij} + \frac{2\zeta^2 R_{ij}^2}{5} + \frac{\zeta^3 R_{ij}^3}{15} \right) \exp(-\zeta R_{ij}) \quad (10)$$

where  $R_{ij}$  is the interatomic distance in bohrs and  $\zeta$  is an orbital-dependent constant set to 1.5679 for carbon 2p orbitals.<sup>20,21</sup> Equation 9 is a consequence of an orbital overlapping with an identical copy of itself (i.e., it is a normalization integral). Note that both the  $\mathbf{H}$  and  $\mathbf{S}$  matrices are symmetric about the diagonal.

The problem of finding MOs of a polyacene, therefore, reduces to the construction of  $\mathbf{H}$  and  $\mathbf{S}$  and subsequently finding the eigenvalues (MO energies) and eigenvectors (expansion coefficients) from eq 4. Both tasks are easily accomplished for small polyacenes with symbolic algebra software such as Maple<sup>10</sup> and, for much larger systems, with student-written source code.

In the construction of both  $\mathbf{H}$  and  $\mathbf{S}$ , it is helpful to distinguish atomic interactions as on-site interactions, bonded interactions (also known as “nearest-neighbor”, NN, interactions, which are bonding interactions between adjacent atoms), second-nearest-neighbor interactions, and higher-order neighboring interactions. These interactions can be indexed by a matrix of dimension  $N \times N$ , where  $N$  is the number of atoms in the molecule. Figure 2 shows the structure of benzene and three such interaction matrices. In a most basic form of EHT, the  $H_{ii}$  and  $S_{ii}$  values are evaluated for on-site interactions, and the  $H_{ij}$  and  $S_{ij}$  elements are evaluated for bonding interactions (e.g., between atoms 1 and 2). Using Figure 2 as a reference, this entails replacing  $a$  with  $H_{ii}$  and  $b$  with  $H_{ij}$  to form the  $\mathbf{H}$  matrix. To form the  $\mathbf{S}$  matrix,  $a$  is replaced with 1, and  $b$  is replaced with  $S_{ij}$ ; the elements that correspond to nonbonding interactions are set to 0, as in Figure 2b. Note that each C–C bond is the same length, so every  $\mathbf{S}$  matrix element corresponding to a bonding interaction will be the same. To make the calculation more sophisticated, second- and third-nearest-neighbor interactions can be incorporated, which gives a more complete picture of the electronic structure of the system. An example of a second-nearest-neighbor interaction would be between atoms 1 and 3, represented by  $c$  in the

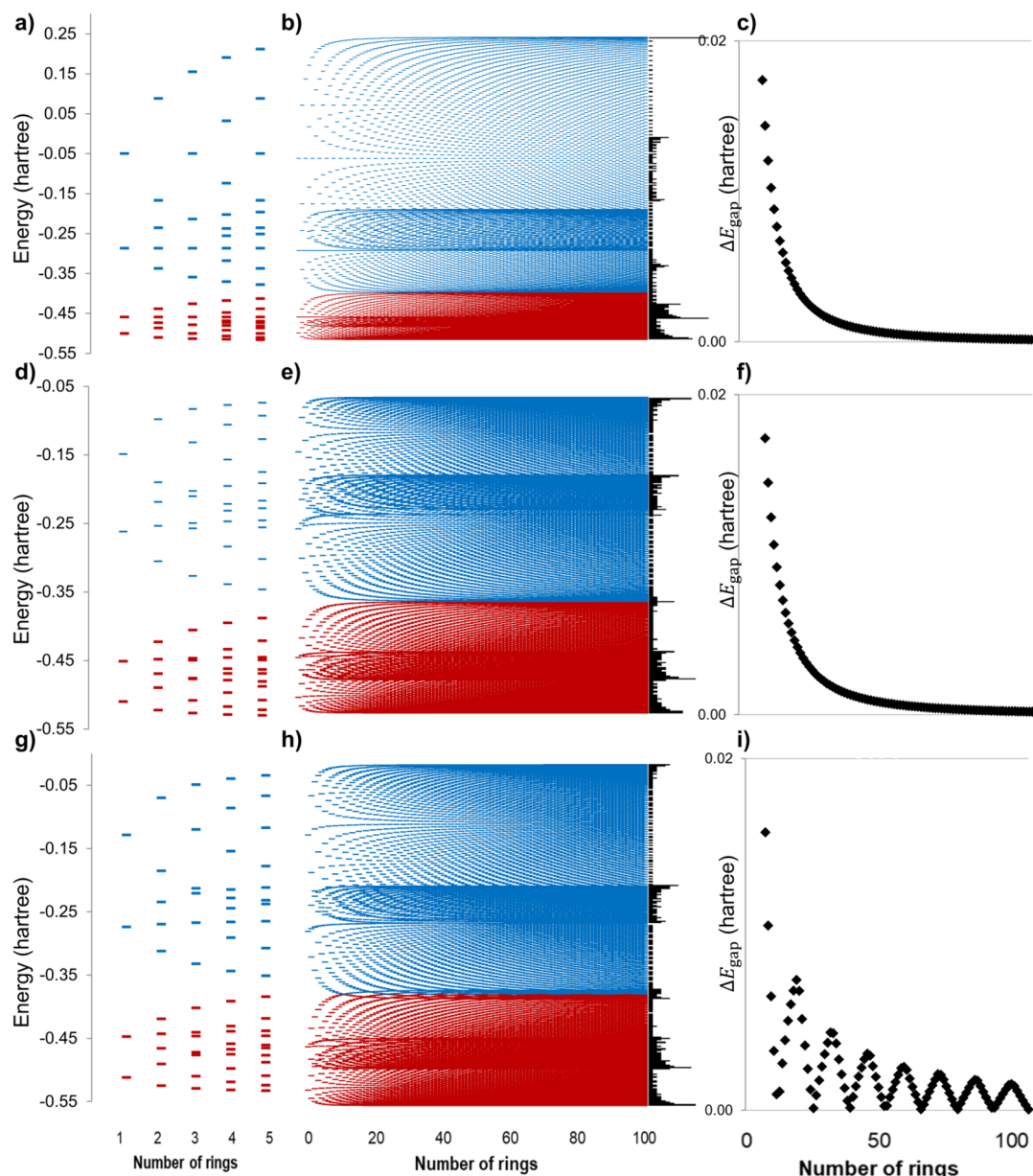


**Figure 3.** Results of the first exercise: (a–c) Set 1, (d–f) Set 2, and (g–i) Set 3. Occupied orbitals are shown in red, whereas virtual orbitals are shown in blue. (b,e,h) To the right are histograms of the densities of states for each system, wherein the longest bar corresponds to a frequency of 15.  $\Delta E_{\text{gap}}$  is the HOMO–LUMO gap computed using eq 12.

interaction matrix (Figure 2c), and a representative third-nearest-neighbor interaction is one between atoms 1 and 4, denoted by  $d$  in the interaction matrix (Figure 2d).

To explore the influence of long-range interactions, three sets of 100 calculations each are performed. Each set contains calculations for the 100 smallest polyacenes from 1 ring (benzene) to 2 rings (naphthalene) up to  $M = 100$  rings. In the first set, only on-site interactions and first-nearest-neighbor interactions are included, with all other interactions set to 0; this is referred to as Set 1. For Set 2, all second-nearest-neighbor interactions along with on-site interactions and first-nearest-neighbor interactions are included. Finally, Set 3 includes all on-site interactions and first-, second-, and third-nearest-neighbor interactions. For each set of calculations, all further interactions (fourth-nearest-neighbors and further), which are present in systems larger than benzene, are set to 0.

Once  $\mathbf{H}$  and  $\mathbf{S}$  are constructed, solving eq 4 yields an  $N \times N$  matrix of eigenvectors and a corresponding  $N$ -component vector of energy eigenvalues. (Effectively, one finds the generalized eigenvalues and eigenvectors of  $\mathbf{H} - \mathbf{S}$ . These eigenvalues are the orbital energies used in the construction of orbital energy level diagrams.) Each eigenvector is made up of expansion coefficients, which describe the molecular orbitals as a linear combination of the AOs. For example, in the case of the  $\text{H}_2$  molecule, students studying linear combinations of atomic orbitals (LCAO) theory will learn that the 2 hydrogen 1s orbitals yield two  $\text{H}_2$  molecular orbitals. One molecular orbital is the algebraically symmetric combination of substituent orbitals; that is, all of the coefficients will share the same sign. In the case of  $\text{H}_2$ , this yields a geometrically symmetric orbital, the “bonding” orbital. Alternatively, the “antibonding” orbital is described by coefficients that alternate

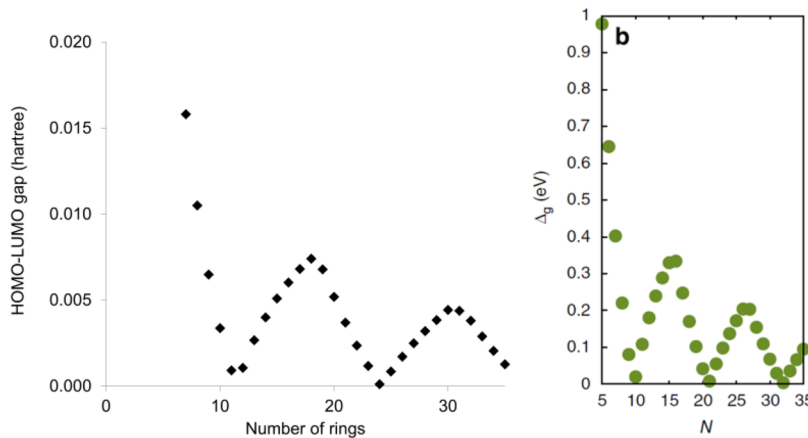


**Figure 4.** Results of EHT computations (left) and PBE computations from ref 13 (right). In the image on the right,  $N$  is the number of rings (denoted  $M$  in the present work) and  $\Delta_g$  is the HOMO–LUMO gap. Reprinted by permission from Springer Nature, *Nat. Comm.*, Signature of the Dirac Cone in the Properties of Linear Oligoacenes, Korytár et al., Copyright 2014.

in sign; that is, it is geometrically and algebraically antisymmetric in the case of  $H_2$ .

Once energy level diagrams are constructed for each system and for each set, it is possible to explore the evolution of the energy of the HOMO–LUMO gap with system size. First, to identify the occupied orbitals, the  $\pi$  electrons in each system, the number of which is denoted  $n$ , are assumed to occupy the  $\frac{n}{2}$  lowest energy orbitals (i.e., the system is taken to be in the ground electronic state). This is easily done by sorting the elements of the eigenvalue vector ( $E$ ) from lowest to highest and indexing them accordingly. It follows that

$$\begin{aligned} E_{\text{HOMO}} &= E_{n/2} \\ E_{\text{LUMO}} &= E_{(n/2)+1} \end{aligned} \quad (11)$$

where each index must be an integer, and the lowest-energy index is 1. For example, the HOMO of benzene is the third-lowest energy level (index = 3), which houses the two highest energies of its six  $\pi$ -electrons. Therefore, the LUMO is the fourth-lowest energy level (index = 4). This means that the energies associated with these orbitals are the third and fourth lowest energies, respectively. The HOMO–LUMO gap energy is computed by taking the difference in energy of the HOMO and LUMO.

$$E_{\text{LUMO}} - E_{\text{HOMO}} = \Delta E_{\text{gap}} \quad (12)$$

By carrying out the full procedure for systems of increasing  $M$ , students will see how orbitals converge into bands at large  $M$  and, specifically, how the system goes from gapped to metallic with no band gap. Upon careful inspection of the resultant molecular orbital energies and the energies of the HOMO–LUMO gap for each set, students can also see the effect of the incorporation of long-range interactions on the electronic structure and HOMO–LUMO gap of the system.

Energy level diagrams for each of the first 100 polyacenes can be constructed using the results of eq 4 with assignment of occupied and virtual orbitals as described above. Figure 3 shows example results for Set 1 along the first row of panels, those for Set 2 along the second row, and those for Set 3 along the third. The leftmost column of panels in Figure 3 shows the energy level diagrams for the first five systems on their own plot for clarity. The center panel of Figure 3 shows the evolution of the energy levels as size is varied from 1 to 100

rings, with the accompanying density of states histograms on the right. Finally, the rightmost panel shows the trend in the HOMO–LUMO gap as size is increased.

The problem statement for Exercise I is as follows: “Create an energy level diagram for the frontier orbitals of each of the 100 smallest polyacenes. Observe the trends with increasing  $M$ .”

The steps for students to perform this exercise are as follows:

- (1) Specify the number of rings ( $M$ ) in the system.
- (2) Select the degree of interaction to be incorporated (i.e., first NN, second NN, or third NN).
- (3) Define the system’s geometry.
- (4) Fill each element of  $\mathbf{H}$  and  $\mathbf{S}$  using eqs 6, 7, 9, and 10.
- (5) Solve eq 4 for eigenvalues and eigenvectors.
- (6) Order the elements of the eigenvalue vector from lowest to highest, determine orbital occupancies, and use the data to generate an energy-level diagram (like Figure 3a,b).
- (7) Compute the HOMO–LUMO gap.
- (8) If the number of rings in the system is below the maximum desired, increment the number of rings by 1 and return to Step 3.
- (9) Generate a graph of the HOMO–LUMO gap versus  $M$  (like Figure 3c).

An example Maple worksheet is included in the [Supporting Information](#) for instructor reference. This sheet employs a complex looping structure to produce results for a wide range of polyacenes but can be used to generate a “key” for what the student results should be for a subset of the small polyacene systems.

### Exercise I Solution Discussion

Figure 3a,d,g shows that there is a general increase in orbital splitting upon incorporation of more interactions. Figure 3b,e,h shows that the high-order interactions are important for the formation of a conduction “band”. These plots themselves can be used as a pedagogical tool to convey the origin of valence and conduction bands in solids. Because there is no discernible gap between the valence band and conduction band at large  $M$ , these figures serve to rationalize why graphene has no band gap and is therefore unsuitable for semiconducting devices like transistors.

Figure 3c,f shows a monotonic decrease of  $E_{\text{gap}}$  as the system size increases from  $M = 1$  to  $M = 100$ . Unsurprisingly, as the orbitals converge into bands, the orbitals become increasingly close in energy to each other. Figure 3i, however, shows that once third-nearest-neighbor interactions are incorporated into the EHT calculations,  $E_{\text{gap}}$  no longer monotonically decreases; it decreases until  $M = 12$ , at which size the gap increases until  $M = 18$ , then decreases until  $M = 24$ , and so on.

Inclusion of third-nearest-neighbor interactions recovers the oscillatory behavior in the HOMO–LUMO gap, which is found at the DFT level of theory using the Perdew–Burke–Ernzerhof (PBE) functional<sup>22</sup> and is indicative of orbital crossing in systems of this type.<sup>13</sup> Results generated using Exercise I are shown in Figure 4 on the left, whereas PBE results from the literature are reproduced on the right. Although EHT does not exactly replicate the values of  $M$  for which the gap is a minimum, these results still imply that in certain size ranges, the HOMO and LUMO of the system will interchange.

This exercise not only shows the evolution of the valence and conduction bands but also demonstrates the profound effect that third-nearest-neighbor interactions can have on the electronic structure of a system. An exercise investigating orbital crossing in stacked dimer systems is described next.

## EXERCISE II: PLOTTING HOMO AND LUMO ENERGIES AS A FUNCTION OF DISPLACEMENT COORDINATE

### Exercise II Background

The second major learning objective and the next level of sophistication is for students to explore how subtle structural changes in layered 2D materials can lead to qualitative changes in the electronic structure. To do so, it is useful to explore the electronic structure of stacked systems of PAHs, which are 2D analogues of polyacenes and thus geometrically similar to graphene.

In the first exercise, described above, students are guided to carry out electronic structure calculations on systems of  $M$  rings using a basis of carbon  $2p_z$  functions. When two such molecules (for example, two benzene rings) are stacked to form a dimer (see Figure 5), however, their bonding is dominated by their HOMOs, so a more appropriate basis for performing a calculation on the benzene dimer system consists of two benzene HOMO functions, one on each monomer. A two-orbital basis will yield  $\mathbf{H}$  and  $\mathbf{S}$  matrices that are each of dimension  $2 \times 2$ . To generate these two basis functions, students may use the expression for the HOMO extracted from the matrix of eigenvectors from the first exercise. For benzene, as stated above, the HOMO is the third-lowest energy level and the expansion coefficients are the elements from the corresponding column of the eigenvector matrix. These coefficients, in conjunction with the  $C\ 2p_z$  basis functions, give molecular orbital functions of the following form:

$$\Phi_{\text{MO}} = \sum_{i=1}^6 c_{h,i} \chi_i = c_{h,1} \chi_1 + c_{h,2} \chi_2 + c_{h,3} \chi_3 + c_{h,4} \chi_4 + c_{h,5} \chi_5 + c_{h,6} \chi_6 \quad (13)$$

where  $h$  denotes the column that represents the HOMO in the eigenvector matrix, and  $i$  indexes the elements of that vector. Equation 13 has six terms because there are six basis functions in the  $C\ 2p_z$  basis for benzene. This eigenvector associated

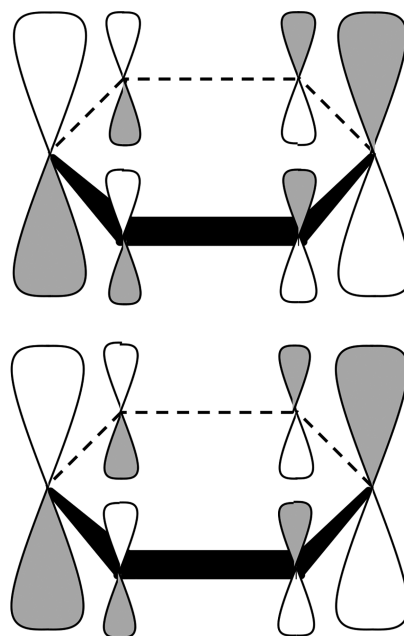


**Figure 5.** Stacked system of benzene rings with the monomer HOMOs superimposed. Each monomer HOMO is a linear combination of  $C\ 2p_z$  atomic orbital functions. A negative expansion coefficient is depicted by the shaded portion of the orbital pointing down; coefficients on one-half of the molecule are positively signed, whereas those on the other half of the molecule are negatively signed. The size of each lobe is proportional to the magnitude of the expansion coefficient, with two dominant AOs at the right- and left-most ends of the molecule.

with the HOMO of benzene can be used to form the basis functions for a calculation on the benzene dimer system, as shown in Figure 5. To do so, one benzene HOMO function is placed on each monomer. Note that the HOMO of a single benzene has a node perpendicular to the plane of the molecule.

For this exercise, the basis is composed of two functions, one monomer HOMO on each layer of the dimer stack. Whereas the subscript  $ij$  indexes atomic interactions, the subscript  $nm$  is used here to index the interaction between monomer HOMOs. To construct the  $\mathbf{H}$  and  $\mathbf{S}$  matrices for this system, eqs 6, 7, and 9 apply, but for clarity, these expressions will be denoted  $H_{nm}$ ,  $H_{nnm}$ , and  $S_{nm}$ , with  $H_{nn}$  being minus the ionization energy of the monomer ( $-9.24$  eV for benzene). This assumption is in the spirit of the MWH approximation, where the atomic VOLE is used to define the diagonal (on-site) energy integral. The  $\mathbf{S}$  matrix elements  $S_{nm}$  are more easily computed by recognizing that the overlap integral of molecular orbitals simplifies to a linear combination of atomic ( $S_{ij}$ ) overlap integrals as follows:

$$\begin{aligned} S_{nm} &= \int \Phi_n \Phi_m \, d\tau = \int \sum_{i=1}^N \sum_{j=1}^N c_{in} c_{jm} \chi_{in}^* \chi_{jm} \, d\tau \\ &= \sum_{i=1}^N \sum_{j=1}^N c_{in} c_{jm} \int \chi_{in}^* \chi_{jm} \, d\tau = \sum_{i=1}^N \sum_{j=1}^N c_{in} c_{jm} S_{ijnm} \end{aligned} \quad (14)$$

where  $N$  is the number of constituent AOs in the expansion of the MO.

For one  $C\ 2p_z$  orbital directly above another one (i.e., coaxial atomic orbitals), the overlap is purely  $\sigma$  in character. Using Figure 5 as reference, however, it can be seen that the

majority of atomic interactions in this stacked dimer system are those of atoms on one monomer interacting in an “oblique” fashion with an atom on the other monomer, a schematic of which is shown in Figure 6.

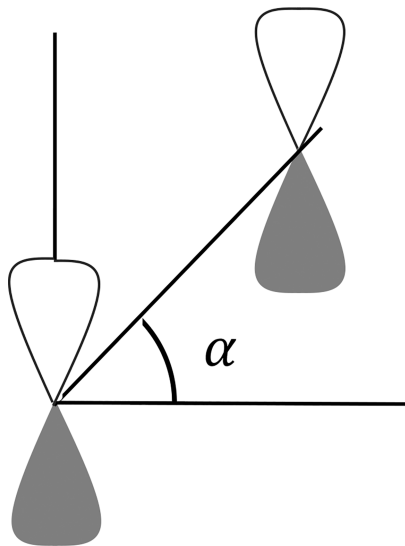


Figure 6. Diagram of oblique overlap of  $p_z$  orbitals.

This oblique overlap is mathematically a combination of  $\pi$  and  $\sigma$  overlap and is described thus (see ref 16):

$$S_{ij_{\text{oblique}}} = (\cos^2 \alpha) S_{ij_{pp_\pi}} - (\sin^2 \alpha) S_{ij_{pp_\sigma}} \quad (15)$$

Here,  $\alpha$  is the angle of offset between the two orbital centers,  $S_{ij_{pp_\pi}}$  is given as eq 10, above, and  $S_{ij_{pp_\sigma}}$  is as follows, where  $R_{ij}$  and  $\zeta$  are defined above:<sup>19</sup>

$$S_{ij_{pp_\sigma}} = \left( -1 - \zeta R_{ij} - \frac{\zeta^2 R_{ij}^2}{5} + \frac{2\zeta^3 R_{ij}^3}{15} + \frac{\zeta^4 R_{ij}^4}{15} \right) \times \exp(-\zeta R_{ij}) \quad (16)$$

Note that in eq 15, the limiting case  $\alpha = 0$  describes  $\pi$  overlap, and  $\alpha = 90$  describes  $\sigma$  overlap with opposite lobes interacting. For that reason, all of the atomic overlaps can be computed using the  $S_{ij_{\text{oblique}}}$  expression. The resulting  $S$  matrix will have ones for the diagonal elements, and the off-diagonal elements will be equal to  $S_{nm}$ , given by eq 14.

For this second exercise, interactions of all atoms within 10 bohr of each other should be included; this ensures the inclusion of third-nearest-neighbor interactions. A distance cutoff, rather than a degrees-of-separation cutoff, is important for this exercise because nearest-neighbors are not fixed when considering monomer–monomer displacement within a dimer.

An advantage to using a basis of two HOMOs ( $n$  and  $m$ ) instead of a basis of  $2N$  C  $2p_z$  orbitals is that the results are easier to interpret; solving eq 4 yields just 2 “stacked” dimer orbitals instead of 12 molecular orbitals. These two stacked molecular orbitals of the dimer system are expressed as linear combinations of monomer HOMOs; their character is given by the elements of the two resultant eigenvectors. As described above, the signs of the elements of the eigenvector denote the character of the interaction. Because the two basis functions each contain a nodal plane coincident with the plane of the

corresponding monomer, and the monomers are stacked in the direction normal to these planes, the eigenvector for which all of the expansion coefficients have the same sign describes an algebraically symmetric but geometrically antisymmetric combination of orbitals. Correspondingly, the eigenvector for which the expansion coefficients alternate in sign describes an algebraically antisymmetric but geometrically symmetric combination. Because the geometric symmetry determines the relative energies of two orbitals, the “stacked” orbital that corresponds to the algebraically symmetric combination of basis functions, then, is actually the higher-energy orbital, whereas the antisymmetric combination is lower in energy. This offers a contrast to the “bonding” and “antibonding” picture taught in general chemistry courses, wherein the bonding combination is typically a symmetric combination of atomic orbitals and the antisymmetric combination yields an antibonding molecular orbital. The energetic relationship between these two stacked monomer orbital contributions to the dimer orbitals is used to introduce students to  $k$ -space and band crossing, below. Using eqs 9 and 15 along with eqs 14, 10, and 16, students can determine the HOMO–HOMO overlap integral to construct the  $2 \times 2$   $S$  matrix for a dimer system. The  $H$  matrix is then constructed using the MWH approximations outlined above. The energies of the two stacked orbitals of the dimer are then determined by solution of eq 4.

Once the framework is in place for studying the electronic structure of these systems using EHT, students can use this procedure to explore the implications of layer–layer offset or turbostratic disorder<sup>23</sup> in these bilayer materials. Three types of disorder, “stretching”, “sliding”, and “twisting”, are shown in Figure 7.

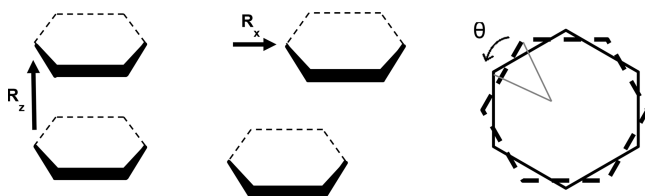
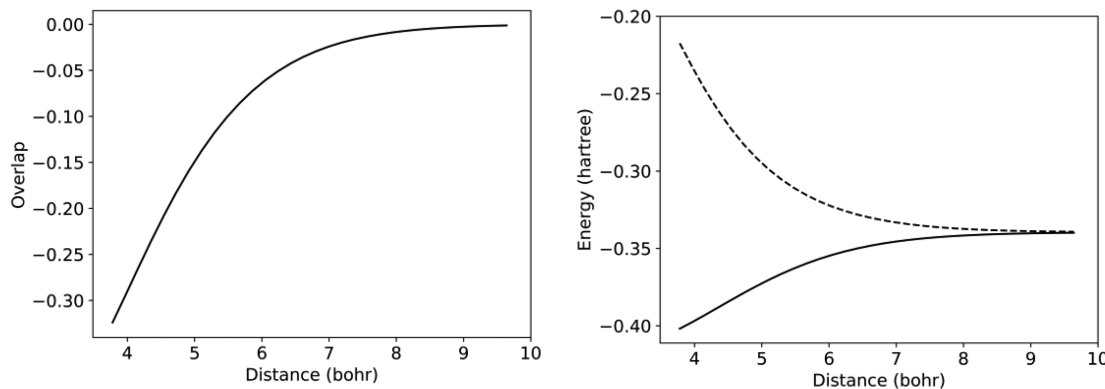
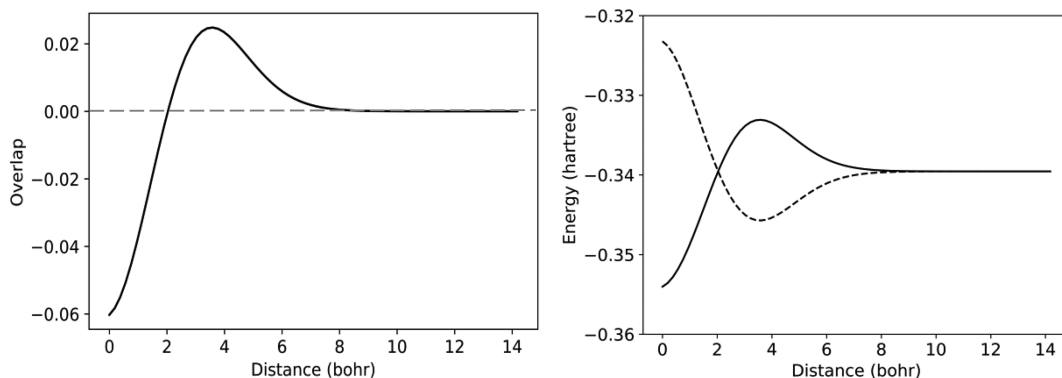


Figure 7. Three types of displacement explored in Exercise II: stretching (left), sliding (center), and twisting (right), using a system of two benzene rings as an example, with orbitals redacted for clarity (see Figure 5).

A benzene dimer can provide basic insight into the electronic structure of layered materials, but for a more complete model, dimers of larger monomers can be investigated using the same framework. For this reason, example results, in addition to benzene, are shown here for twisting of dimer structures of coronene, circumcoronene, and a 1261-ring PAH system (of the same symmetry). Whereas coronene and circumcoronene have 3 and 5 rings along their longest axes, respectively (see structures II and III of Figure 1), this 1261-ring system has 41 rings along the longest axis. This largest system approximates graphene, so for the diagonal elements of  $H$  ( $H_{nn} = -IE_{\text{molecule}}$ ), the ionization energy of graphene,  $-4.57$  eV, is used.<sup>24</sup> In the example solutions shown here, for twisting calculations on the benzene dimer, one of the molecules is twisted through the range of  $0$ – $180^\circ$  with respect to the other; for the larger systems, twisting is performed through  $0$ – $90^\circ$  for computational efficiency.



**Figure 8.** Overlap integral (left) and stacked orbital energies (right) vs  $R_z$  for a benzene dimer. The energy of the orbital that represents the algebraically symmetric combination of orbitals is represented by a dashed line; that of the antisymmetric one is represented by a solid line. For all graphs, the width of a data point is comparable to the diameter of a line.



**Figure 9.** Overlap integral (left) and stacked orbital energies (right) vs  $R_x$  for a benzene dimer. The overlap changes sign and the energy levels cross around  $R_x = 2.04$  bohr. In the plot on the left, a dashed line is shown where the overlap equals 0 for reference. In the plot on the right, the energy of the orbital that represents the algebraically symmetric combination of orbitals is represented by a dashed line; that of the antisymmetric one is represented by a solid line.

The problem statement for Exercise II is as follows: “Plot the HOMO and LUMO energies as a function of stacking distance for stacked dimers of several PAHs. Repeat for slip displacement and twist disorder.”

The steps for students to perform this exercise are as follows:

- (1) Specify a ring system to use as a monomer (benzene, coronene, etc.).
- (2) Generate values for  $c_{h,i}$  using Exercise I.
- (3) Define the geometry of the dimer system.
- (4a) Construct  $S$  using eqs 9 and 14. (If  $R_{ij} > 10$  bohr,  $S_{ij} = 0$ .)
- (4b) Store the value of  $S_{nm}$  for plotting.
- (5) Construct  $H$  using eqs 6 and 7, where  $H_{mn} = -IE_{\text{molecule}}$ .
- (6a) Solve eq 4.
- (6b) If the two components of the first eigenvector have the same sign, append the first energy to an “algebraically symmetric” orbital list. If they have different signs, append to an “algebraically antisymmetric” orbital list. Append the second energy to the other list.
- (7) Alter geometry by stretching, sliding, or twisting, and return to Step 3.
- (8) Generate graphs of overlap integral versus  $R_z$ ,  $R_x$ , and  $\theta$  and energy versus  $R_z$ ,  $R_x$ , and  $\theta$  for the system.

#### Exercise II Solution Discussion

**“Stretching” a Benzene Dimer.** Figure 8 shows an example plot of the overlap of monomer HOMOs (left) and

dimer orbital energies (right) as  $R_z$  changes from 2 to 5 Å. At small  $R_z$  distances of separation, the monomer HOMOs interact strongly, and the two dimer orbitals have a large energy difference. As the distance between the two benzene rings increases, the overlap approaches 0, and the dimer orbitals converge to be the same energy level, which is that of the HOMO of an isolated monomer. These results should be intuitive to students as they are reminiscent of H 1s AO interactions in H<sub>2</sub>, as presented in a General Chemistry course.

**“Sliding” a Benzene Dimer.** To consider the effect of sliding on the electronic structure, the dimer system is constructed as before, this time with the layer–layer spacing held constant at 3.2 Å, consistent with the interlayer spacing in graphite.<sup>25</sup> As one benzene ring “slides” with respect to the other, at a value of  $R_x \approx 2.04$  bohr (1.08 Å), a change in the sign of the overlap occurs, because at this distance, positive contributions to the overlap begin to dominate the system. The corresponding energy level versus distance plot (Figure 9 right) first shows the two energetically different orbitals coming closer in energy until they appear to cross at the value of  $R_x$  where the overlap integral changes sign. Figure 10 shows the corresponding geometry at  $R_x \approx 2.04$  bohr. At  $R_x = 3.59$  bohr (1.90 Å), the orbital splitting reaches a local maximum or minimum, and they converge to be energetically equivalent at a large sliding distance where the monomers are essentially noninteracting, as in the stretching case. Note that students

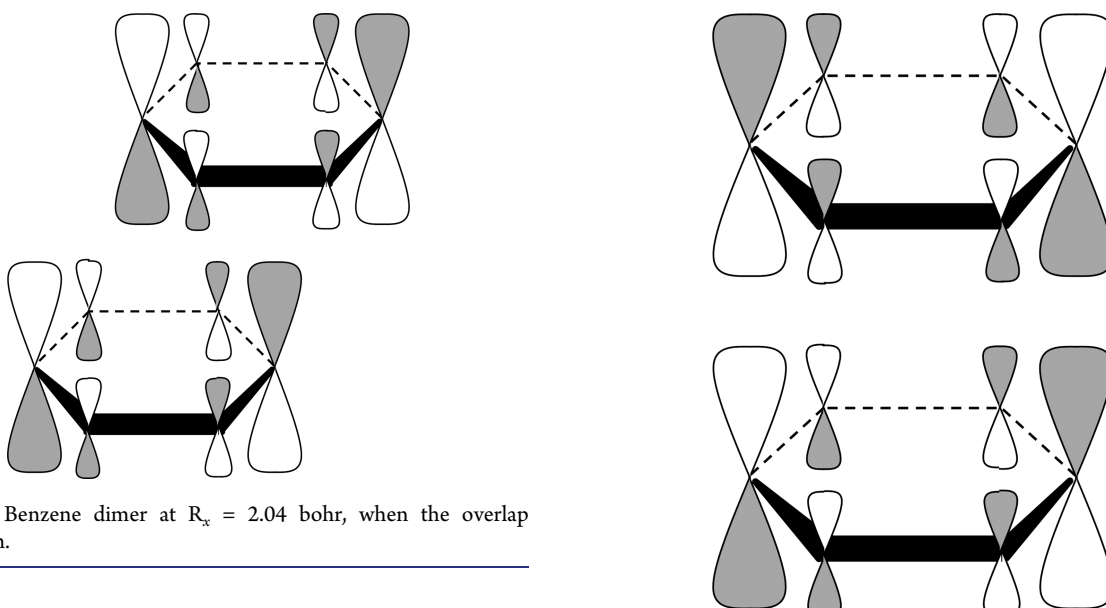


**Figure 10.** Benzene dimer at  $R_x = 2.04$  bohr, when the overlap changes sign.

should ensure that they are performing sliding in the direction that is perpendicular to the node of the monomer HOMO.

**“Twisting” a Benzene Dimer.** A twisting motion can be considered a combination of translational motions, and when one ring system is twisted with respect to the other, an oscillation in the sign of the overlap integral is observed.

As shown in Figure 11 for benzene at a twist angle of  $\theta = 90^\circ$ , the value of the overlap of the system reaches 0, and the energy levels cross. At a twist angle of  $\theta = 180^\circ$ , the overlap reaches a positive maximum (see Figure 12).

Graphs of overlap integral versus twist angle and energy level versus twist angle are shown in Figures 13–15 for each benzene, coronene, circumcoronene, and “graphene” dimer system.

As the number of rings in the system grows, the frequency of overlap sign change increases, and energy level crossings occur more frequently. Not coincidentally, as the size of the system increases, the first crossing instance occurs sooner.

In a calculation where a much larger system is considered (a dimer with monomers consisting of 101 rings along the longest side), the first crossing occurs at an offset angle near  $1^\circ$ , as shown in Figure 16. This calculation is exceedingly computationally expensive and is included here for completeness,

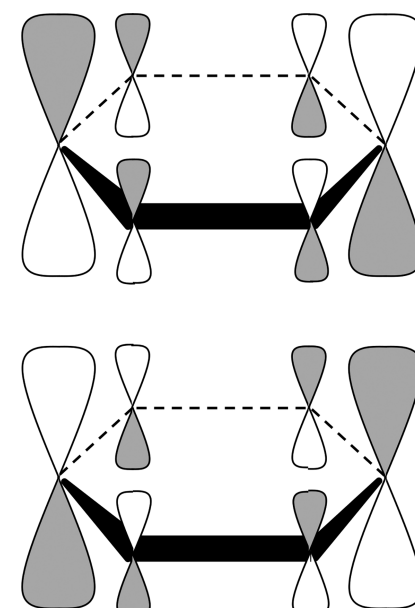


**Figure 12.** Benzene dimer at a twist angle of  $180^\circ$ , where the overlap is at a maximum. Note that all purely  $\sigma$  overlaps are positive, in contrast to Figure 5. The orbitals cross at a twist angle of  $90^\circ$ .

without the expectation that it would be carried out by students.

#### Effect of Orbital Crossing on the Band Structure of Bilayer Graphene

It has been shown that a change in the sign of the overlap can have important implications for the electronic properties of stacked materials.<sup>26</sup> A consequence of this overlap sign change and orbital crossing is explored next.

Band structure plots are often seen in materials literature and can be initially confusing to chemistry students. A band structure plot is a plot of energy versus spatial frequency,  $k$ . The point  $k$ , termed the “gamma point” is labeled  $G$  or  $\Gamma$  and shows the energy associated with the eigenvector that represents the symmetric combination of orbitals. Therefore, the energy calculations described in each of these exercises above represent gamma-point calculations of PAH dimers.

By applying the concept of  $k$ -space to the results of this exercise, students can be led to the root of the sensitivity of the

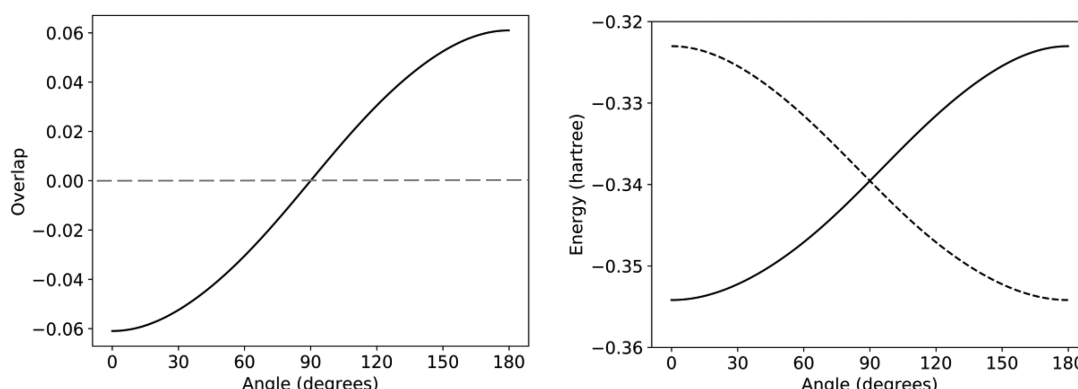


**Figure 11.** Overlap integral (left) and energy (right) vs  $\theta$  for a benzene dimer. The overlap changes sign and the energy levels cross once, at a  $90^\circ$  twist angle. In the plot on the left, a dashed line is shown where the overlap equals 0 for reference. In the plot on the right, the energy of the orbital that represents the algebraically symmetric combination of orbitals is represented by a dashed line; that of the antisymmetric one is represented by a solid line.

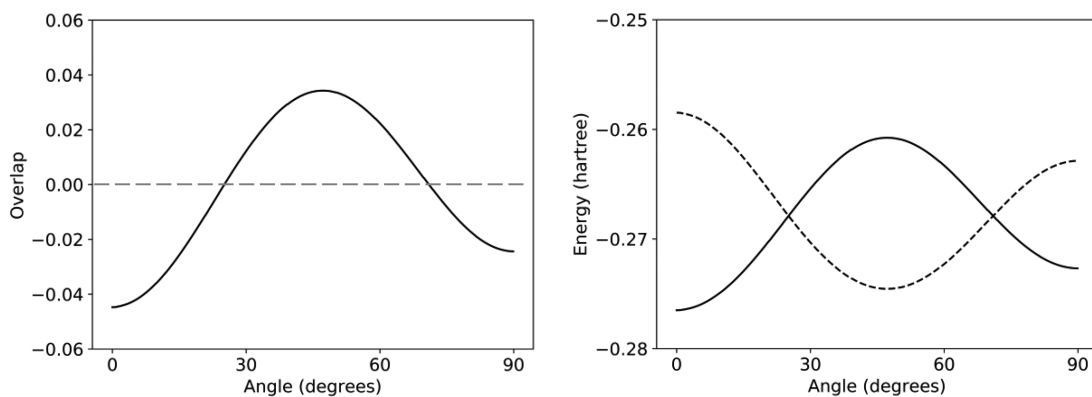


**Figure 13.** Overlap integral (left) and energy (right) vs  $\theta$  for a coronene dimer. The structure of coronene is shown in Figure 1 (structure II). The overlap changes sign and the energy levels cross twice, at about 25.1 and 71° twist angles. In the plot on the left, a dashed line is shown where the overlap equals 0 for reference. In the plot on the right, the energy of the orbital that represents the algebraically symmetric combination of orbitals is represented by a dashed line; that of the antisymmetric one is represented by a solid line.

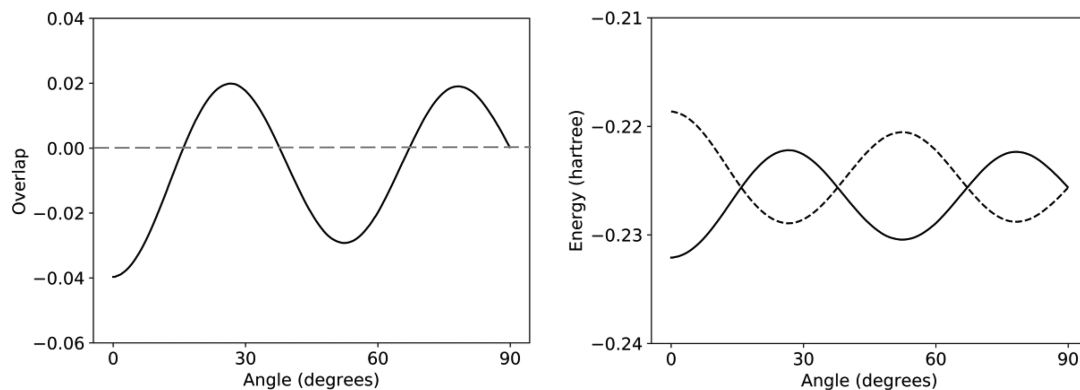


**Figure 14.** Overlap integral (left) and energy (right) vs  $\theta$  for a circumcoronene dimer. The structure of circumcoronene is shown in Figure 1 (structure III). The overlap changes sign and the energy levels cross four times, at 15.9, 37.7, 67.1, and 90° twist angles. In the plot on the left, a dashed line is shown where the overlap equals 0 for reference. In the plot on the right, the energy of the orbital that represents the algebraically symmetric combination of orbitals is represented by a dashed line; that of the antisymmetric one is represented by a solid line.

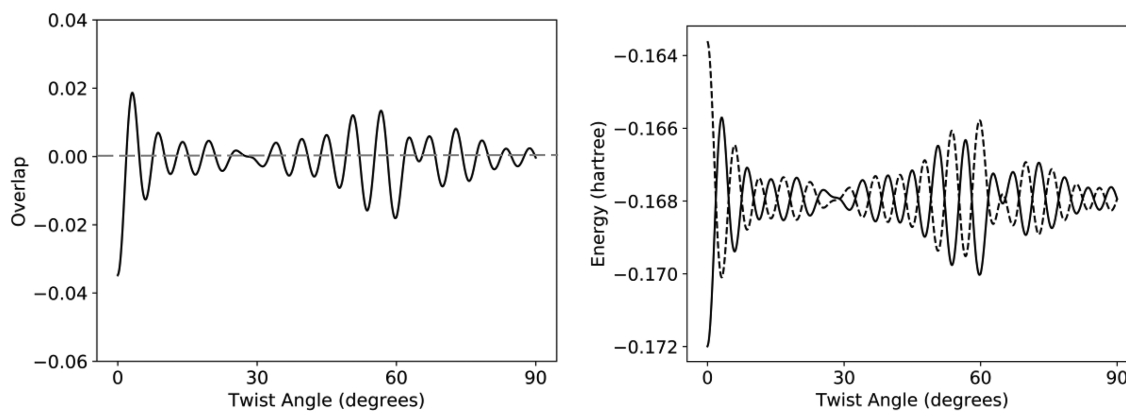


**Figure 15.** Overlap integral (left) and energy (right) vs  $\theta$  for a “graphene” dimer. The overlap changes sign and the energy levels cross many times. In the plot on the left, a dashed line is shown where the overlap equals 0 for reference. In the plot on the right, the energy of the orbital that represents the algebraically symmetric combination of orbitals is represented by a dashed line; that of the antisymmetric one is represented by a solid line.

electronic structure to the geometric structure in bilayer 2D materials. To introduce  $k$ -space, the MO picture is first revisited. As mentioned above, the coefficients in an eigenvector describe the bonding character of the orbital. In a solid, suppose there is just one basis function per unit cell. (This is analogous to one basis function per monomer in a stack, as in the previous section.) The top/bottom of a band

will be the entirely symmetric combination of the constituent basis functions (i.e., coefficients signed +++++++...), whereas the bottom/top of the band will be the entirely antisymmetric combination (i.e., coefficients signed +-+-+--...). If there are more than two monomers in a stack, all other linear combinations of monomer HOMOs (e.g., coefficients signed +-+-+...) will fall between these two energy extremes, and

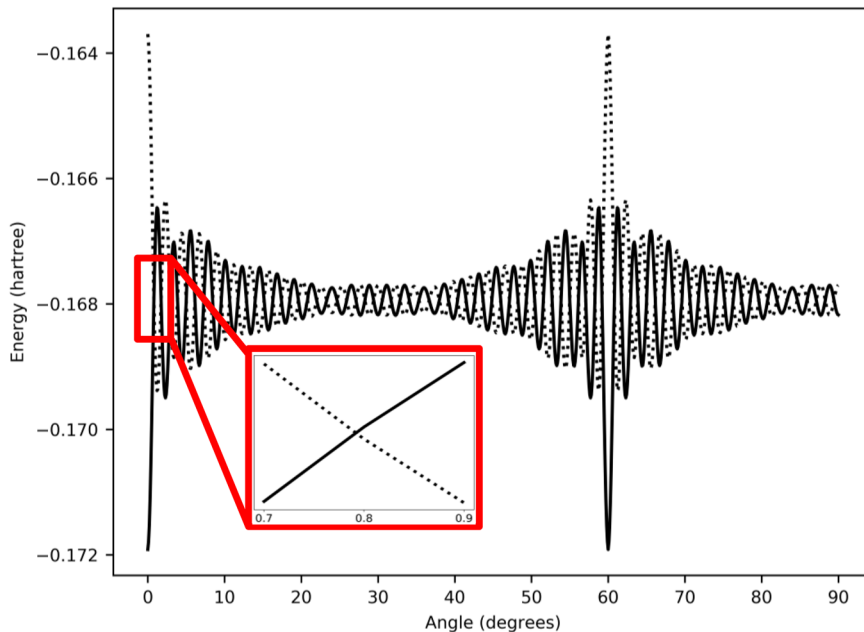


**Figure 16.** Energy vs  $\theta$  for the two stacked orbitals of the larger “graphene” dimer. The inset shows that the energy levels cross many times, with the first occurrence at  $\theta \approx 1^\circ$ . The energy of the orbital that represents the algebraically symmetric combination of orbitals is represented by a dashed line; that of the antisymmetric one is represented by a solid line.

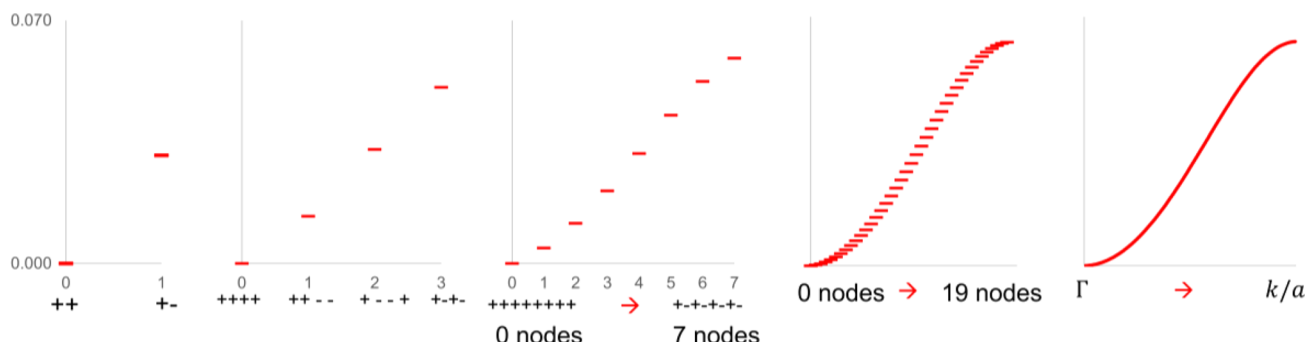


**Figure 17.** Orbital energies for finite stacks of (a) 2, (b) 4, (c) 8, and (d) 40 molecules and for (e) infinite stack of benzene monomers. The fully geometrically symmetric combination of monomer basis functions define the bottom of the band; these are denoted by the succession of “+” marks. The fully antisymmetric combination of functions define the top of the band; these are denoted by the succession of “-” marks, one of which represents two orbitals with a node in between them. As the number of monomers increases, the orbitals fill in the energy space between these two extremes until, in the infinite limit, band energy may be expressed as a function of the spatial frequency of sign changes. In each graph, the energy values have been normalized such that the lowest energy eigenvalue is 0.

thus their energies can be thought of as a discrete function of the frequency of sign changes in the associated expansion coefficients. As the number of repeat units increases, the number of independent linear combinations of basis functions becomes higher, and these intermediate-energy MOs begin to fill in the energy space and create “bands” in between the maximum bonding and maximum antibonding extremes (see Figure 17). In the limit of a macroscopic material, there are effectively infinitely many repeat units ( $\sim 10^{23}$ ). The band energies are a continuous function of the spatial frequency of the corresponding wave function,  $k = 2\pi/\lambda$ , where  $\lambda$  is the wavelength. With one basis function per unit cell, the highest possible spatial frequency is  $k = 2\pi/a$  (i.e., the sign changes every unit cell). At half this frequency, the sign changes every two unit cells. When  $k = 0$ , the sign never changes. Note that  $k$  has units of reciprocal distance. This makes  $k$  effectively a way to index the number of wavelengths per distance (i.e., it is a continuous way to count nodes or sign changes);  $k$  is the

continuous limit of counting nodes per unit distance. It is especially relevant when the system contains a repeat unit, or it is a stack or a chain of molecules. One can therefore define a function,  $E(k)$ , that specifies how the band energy varies from the  $k = 0$  bonding extreme to the  $k = \pi/a$  antibonding extreme. The authors recommend ref 27 for a more complete description.

The curvature of the bands in  $k$ -space tells about the electronic properties of the system. When the overlap is strong, the bandwidth is large, and the energy change with  $k$  exhibits a steeper slope, whereas flat bands in  $k$ -space indicate weak overlap between the orbitals. In bilayer benzene, when one benzene ring is twisted with respect to the other from  $0^\circ < \theta < 90^\circ$ , as shown in Figure 11 above, the symmetric combination of orbitals is the highest energy level for the system, so at small deviations from  $k$ , students can expect to see the energy of the band decrease with  $k$  (toward the energy of the other orbital). With increasing angle, after the crossing occurs at  $90^\circ$ , this

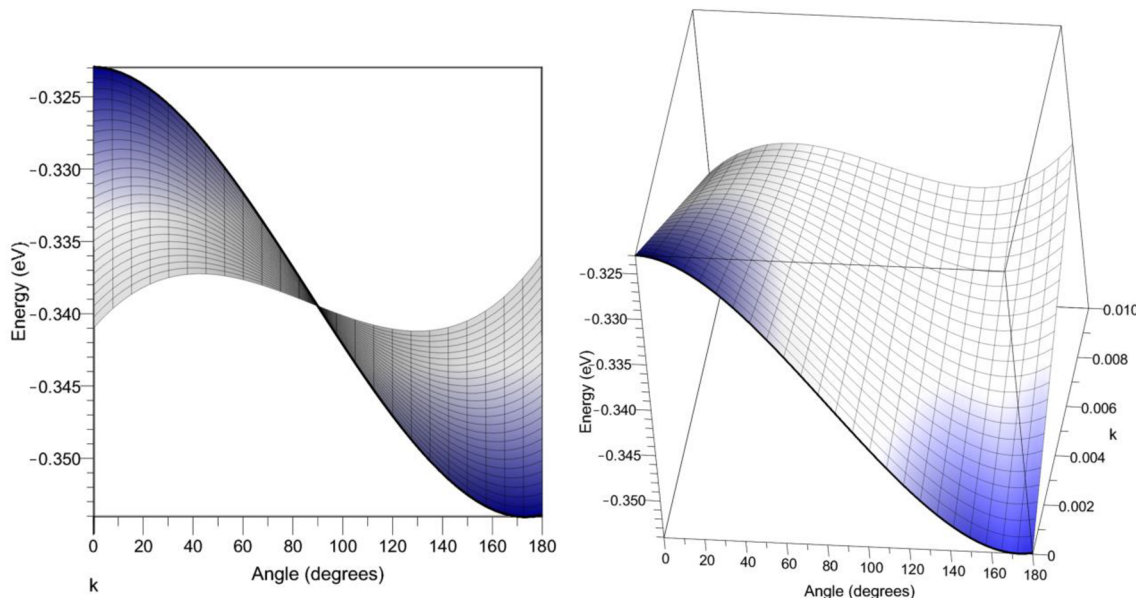


**Figure 18.** Energy vs  $\theta$  and  $k$  for the two stacked orbitals of the benzene dimer. The bands are flat at the crossing point of  $90^\circ$ .

symmetric combination is now the lower-energy orbital, so now the band energy will increase with  $k$ . This knowledge allows students to develop a broader picture of the energy versus angle plots above. At small deviations from the gamma point, the energy of the symmetric band will vary with  $k$  toward the energy of the orbital that represents the entirely antisymmetric combination of constituent orbitals.

Figure 18 shows a schematic of the effect of the twisting angle on the variation in band energy from the results for the benzene dimer (Figure 11). Before and after the crossing point at  $90^\circ$ , the band that results from the combination of monomer HOMOs has some definitive width that will make the bands vary with  $k$ . At the crossing point at  $90^\circ$ , the HOMO band must now be flat in  $k$ -space because the width of the band is exceedingly small. See the *Supporting Information* for a video version of Figure 18.

With the above insight, it can be rationalized that the band structure of the material can vary dramatically within a small range of angle; this range of angle becomes narrower as the size of the system increases, with graphene representing the upper limit of size. Recent literature has shown that the bands of bilayer graphene become flat when the “magic angle” between the two layers is  $1.1^\circ$  (see ref 15 and the supplementary video within); other possible “magic angles” follow a periodicity related to the symmetry of the system.<sup>28</sup> The appearance of flat bands has since been related to superconductivity in bilayer graphene and related systems.<sup>29</sup> Although the level of theory used in the activity described here cannot predict superconductivity, it can reveal the origin of the dramatic dependence of electronic structure on the geometric structure. The results that students achieve while performing Exercise II show why the bands are flat in  $k$ -space: because of sign changes in the overlap of the two stacked monomer orbitals. This exercise therefore serves as a starting point for understanding how rotation through a small range of twist angles can induce dramatic changes in the electronic structure of a system.

## ■ TRUNCATED VERSIONS OF EXERCISES I AND II

For Exercise I, the authors note that a student can perform calculations for  $M = 1$  through  $M = 15$  or 25 and retain the

pedagogical purpose of the exercise. This is valuable because calculations for the smaller systems are easily carried out with symbolic algebra software such as Maple,<sup>10</sup> so knowledge of a formal programming language is not required. For Exercise II, students can perform only stretching and sliding calculations on the benzene dimer system and be able to see orbital crossing; this system is small, and these displacements do not require the use of a rotational matrix. Figure 18 can be presented in lecture when discussing results. Twisting calculations can be performed on the benzene, coronene, and circumcoronene dimer systems, because students will be able to see the trend in the consequences of overlap as size increases with these less expensive computations. Students with more advanced programming knowledge, for example, students pursuing theoretical chemistry, may be motivated to perform the entire study described in this work.

## ■ CONCLUSIONS

Graphene is a modern material with intriguing and potentially technologically valuable electronic structure properties. Presented here are two exercises that teach about the electronic structure of graphene but can also serve as a vehicle for teaching fundamental ideas in the electronic structure of materials, such as the relationship of electronic bands in materials to molecular orbitals, the concept of  $k$ -space, and the origins of band curvature in  $k$ -space. In the first exercise, extended Hückel molecular orbital theory is used to calculate the energy levels and HOMO–LUMO gaps of a system of polyacenes of increasing size. This electronic structure model is sufficiently simple for student use yet captures enough of the basic physics and chemistry to convey the concepts behind electronic structure. Observing the evolution of the molecular orbital diagram with system size reveals how molecular orbitals converge into bands in extended materials. By incorporating more off-diagonal matrix elements, students can learn how long-range interactions influence the overall electronic structure. More complex calculations can be employed in order to teach about how orbital interactions are related to band curvature in  $k$ -space. It is also an excellent exercise to reinforce key programming concepts, such as looping and

variable indexing, although the use of algebraic manipulation software is also appropriate.

## ■ ASSOCIATED CONTENT

### § Supporting Information

The Supporting Information is available on the ACS Publications website at DOI: [10.1021/acs.jchemed.9b00331](https://doi.org/10.1021/acs.jchemed.9b00331).

Maple worksheet for the first exercise, video animating the contents of Figure 18, and comprehensive PowerPoint document with more information about the article contents and suitable for presentation to students in whole or in part ([ZIP](#))

## ■ AUTHOR INFORMATION

### Corresponding Author

\*E-mail: [kws24@drexel.edu](mailto:kws24@drexel.edu).

ORCID 

Janna Domenico: [0000-0002-5825-2994](https://orcid.org/0000-0002-5825-2994)

Alexis M. Schneider: [0000-0002-2158-6915](https://orcid.org/0000-0002-2158-6915)

Karl Sohlberg: [0000-0002-9537-4691](https://orcid.org/0000-0002-9537-4691)

### Present Address

<sup>†</sup>A.M.S.: Department of Biological Engineering, Massachusetts Institute of Technology, Cambridge, Massachusetts 02139-4307, United States

### Notes

The authors declare no competing financial interest.

## ■ ACKNOWLEDGMENTS

The authors gratefully acknowledge Brian Farrell, Nichole O'Neill, and the CHEM 358 class at Drexel University for valuable feedback on the manuscript and supplementary materials.

## ■ REFERENCES

- (1) Novoselov, K. S.; Geim, A. K.; Morozov, S. V.; Jiang, D.; Zhang, Y.; Dubonos, S. V.; Grigorieva, I. V.; Firsov, A. A. Electric Field Effect in Atomically Thin Carbon Films. *Science* **2004**, *306* (5696), 666.
- (2) Mas-Ballesté, R.; Gómez-Navarro, C.; Gómez-Herrero, J.; Zamora, F. 2D materials: to graphene and beyond. *Nanoscale* **2011**, *3* (1), 20–30.
- (3) Shen, H.; Zhang, L.; Liu, M.; Zhang, Z. Biomedical applications of graphene. *Theranostics* **2012**, *2* (3), 283–294.
- (4) Kemp, K. C.; Seema, H.; Saleh, M.; Le, N. H.; Mahesh, K.; Chandra, V.; Kim, K. S. Environmental applications using graphene composites: water remediation and gas adsorption. *Nanoscale* **2013**, *5* (8), 3149–3171.
- (5) Wang, H.-X.; Wang, Q.; Zhou, K.-G.; Zhang, H.-L. Graphene in Light: Design, Synthesis and Applications of Photo-active Graphene and Graphene-Like Materials. *Small* **2013**, *9* (8), 1266–1283.
- (6) Nordholm, S.; Bäck, A.; Bacskay, G. B. The Mechanism of Covalent Bonding: Analysis within the Hückel Model of Electronic Structure. *J. Chem. Educ.* **2007**, *84* (7), 1201.
- (7) Bahnick, D. A. Use of Hückel Molecular Orbital Theory in Interpreting the Visible Spectra of Polymethine Dyes: An Undergraduate Physical Chemistry Experiment. *J. Chem. Educ.* **1994**, *71* (2), 171.
- (8) Sohlberg, K.; Liu, X. Using Extended Hückel Theory as a Platform To Introduce Jahn-Teller Distortion: The Spontaneous Distortion of 1,3,5,7-Cyclooctatetraene from a Perfect Octagon. *J. Chem. Educ.* **2013**, *90* (4), 463–469.
- (9) Thompson, S. E.; Parthasarathy, S. Moore's law: the future of Si microelectronics. *Mater. Today* **2006**, *9* (6), 20–25.
- (10) *Maple 18*; Maplesoft, a division of Waterloo Maple Inc.: Waterloo, Ontario, Canada, 2018.
- (11) *Mathematica*; Wolfram Research, Inc.: Champaign, IL, 2018.
- (12) Baringhaus, J.; Ruan, M.; Edler, F.; Tejeda, A.; Sicot, M.; Taleb-Ibrahimi, A.; Li, A.-P.; Jiang, Z.; Conrad, E. H.; Berger, C.; Tegenkamp, C.; de Heer, W. A. Exceptional ballistic transport in epitaxial graphene nanoribbons. *Nature* **2014**, *506*, 349.
- (13) Korytár, R.; Xenioti, D.; Schmitteckert, P.; Alouani, M.; Evers, F. Signature of the Dirac cone in the properties of linear oligoacenes. *Nat. Commun.* **2014**, *5*, 5000.
- (14) Katoch, J.; Ulstrup, S.; Koch, R. J.; Moser, S.; McCreary, K. M.; Singh, S.; Xu, J.; Jonker, B. T.; Kawakami, R. K.; Bostwick, A.; Rotenberg, E.; Joziak, C. Giant spin-splitting and gap renormalization driven by trions in single-layer WS<sub>2</sub>/h-BN heterostructures. *Nat. Phys.* **2018**, *14* (4), 355–359.
- (15) Cao, Y.; Fatemi, V.; Fang, S.; Watanabe, K.; Taniguchi, T.; Kaxiras, E.; Jarillo-Herrero, P. Unconventional superconductivity in magic-angle graphene superlattices. *Nature* **2018**, *556*, 43.
- (16) McGlynn, S. P.; Vanquickenborne, L. G.; Kinoshita, M.; Carroll, D. G. *Introduction to Applied Quantum Chemistry*; Holt, Rinehart & Winston: New York, 1972.
- (17) Knippenberg, S.; Starcke, J. H.; Wormit, M.; Dreuw, A. The low-lying excited states of neutral polyacenes and their radical cations: a quantum chemical study employing the algebraic diagrammatic construction scheme of second order. *Mol. Phys.* **2010**, *108* (19–20), 2801–2813.
- (18) Hoffmann, R. An Extended Hückel Theory. I. Hydrocarbons. *J. Chem. Phys.* **1963**, *39* (6), 1397–1412.
- (19) Mulliken, R.; Rieke, C.; Orloff, D.; Orloff, H. Formulas and numerical tables for overlap integrals. *J. Chem. Phys.* **1949**, *17* (12), 1248–1267.
- (20) Clementi, E.; Raimondi, D. L. Atomic Screening Constants from SCF Functions. *J. Chem. Phys.* **1963**, *38* (11), 2686–2689.
- (21) Clementi, E.; Raimondi, D. L.; Reinhardt, W. P. Atomic Screening Constants from SCF Functions. II. Atoms with 37 to 86 Electrons. *J. Chem. Phys.* **1967**, *47* (4), 1300–1307.
- (22) Perdew, J. P.; Burke, K.; Ernzerhof, M. Generalized Gradient Approximation Made Simple. *Phys. Rev. Lett.* **1996**, *77* (18), 3865–3868.
- (23) Mailian, A.; Panosyan, Z.; Yengibaryan, Y.; Margaryan, N.; Mailian, M. Identification of Turbostratic Bilayer Graphene in Carbon Tribolayers. *Am. J. Nano Res. Appl.* **2017**, *5* (3–1), 22–25.
- (24) Yu, Y.-J.; Zhao, Y.; Ryu, S.; Brus, L. E.; Kim, K. S.; Kim, P. Tuning the Graphene Work Function by Electric Field Effect. *Nano Lett.* **2009**, *9* (10), 3430–3434.
- (25) Chen, X.; Tian, F.; Persson, C.; Duan, W.; Chen, N.-x. Interlayer interactions in graphites. *Sci. Rep.* **2013**, *3*, 3046.
- (26) Kato, R. Conducting Metal Dithiolene Complexes: Structural and Electronic Properties. *Chem. Rev.* **2004**, *104* (11), 5319–5346.
- (27) Albright, T. A.; Burdett, J. K.; Whangbo, M.-H. *Orbital interactions in chemistry*; John Wiley & Sons, Inc.: Hoboken, NJ, 2013.
- (28) Tarnopolsky, G.; Kruchkov, A. J.; Vishwanath, A. Origin of Magic Angles in Twisted Bilayer Graphene. *Phys. Rev. Lett.* **2019**, *122* (10), 106405.
- (29) Marchenko, D.; Evtushinsky, D. V.; Golias, E.; Varykhalov, A.; Seyller, T.; Rader, O. Extremely flat band in bilayer graphene. *Sci. Adv.* **2018**, *4* (11), No. eaau0059.